ACS OMEGA

Open Access

http://pubs.acs.org/journal/acsodf

Article

Formation of Self-Assembled Nanowires from Copper Nanoparticles Synthesized by the Electro-Explosion of Wires Technique—Study of the Time-Dependent Structural and Functional Evolution

Ranjita Ghosh Moulick,* Subhavna Juneja, Jagriti Gupta, Vaishali Rana, and Jaydeep Bhattacharya

Cite This: *ACS Omega* 2023, 8, 46481−46489

Read Online

ACCESS | Metrics & More | Article Recommendations | Supporting Information

ABSTRACT: We report here the formation of Cu nanowires (CuNWs) from Cu nanoparticles (CuNPs) by a self-assembly process. The CuNPs were synthesized by the electro-explosion of wire (EEW) technique that included nonequilibrium processes for the synthesis. Structural evolution in terms of aggregation or nanowire formation in the samples was observed when the CuNPs were kept for a month after synthesis in a glass vial without the application of any external driving force. The emergence of tangled CuNWs was noticed at the bottom of the vials only when no agitation or aeration was allowed. The nanowires were characterized using transmission electron microscopy (TEM) and X-ray diffraction (XRD). Thermal oxidation of the nanowire samples implied that they could convert into rod-shaped structures. Loss of functionality was also observed in the hemoglobin precipitation study conducted to compare the activity of freshly prepared CuNPs and CuNWs. From the above observations, we conclude that the CuNP, after synthesis, possesses a huge amount of energy, and attainment of equilibrium occurs through either aggregation (clustering) or ordered self-assembly, depending on the conditions applied.

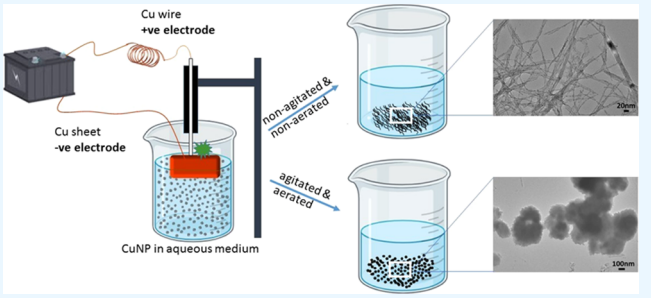

I. INTRODUCTION

The electro-explosion of wire (EEW) technique is associated with the synthesis of monodispersed and highly pure nanoparticles by exploding thin, conductive metal wires. In this process, a high current density pulse (supplied by a capacitor) is carried across a thin conductive metal wire (such as copper), which results in the heating and vaporizing of the wire material. It has been observed that the condensation (rapid cooling) of the vapor results in the formation of nanoparticles from the metal wire in use.[1−3] This technique is associated with processes such as the generation of arcs, shock waves, sudden implementation of a huge amount of energy, etc. Although the relation between the injected energy and its effect on the final product formation is still under investigation,[3,4] it is considered that such extreme non-equilibrium conditions will generate unusual properties in the nanoparticles that are produced by this technique.[5] It is observed that the nanoparticles can easily be passivated by embedding gas in the setup chamber[3] or by adding the coating agent in the solution medium.[6−8] Thus, the nanoparticles synthesized by this technique provide an enormous opportunity to study a broad spectrum of different phenomena. In the presented work, we report the formation of Cu nanowires (CuNWs) from the Cu nanoparticles (CuNPs) synthesized using the EEW technique in the presence of Milli-Q (MQ) water as a medium. The MQ water had no stabilizing agents, such as surfactants or surface-functionalizing agents. Therefore, the particles synthesized were bare and had no surface coatings. In our earlier work, we found that these particles could readily combine with molecules such as poly(ethylene glycol) (PEG) or proteins during the first few days from the day of synthesis. They did not require any external agent or surface chemistry for binding.[8] However, this activity of combining other molecules slowed with time, which could be due to the relaxation behavior of the nanoparticles and the formation of oxides (oxygen taken from air or water). In some cases, when the CuNPs were kept for months in the medium without agitation or aeration, the interaction between the moieties led to the formation of self-assembled nanowires (at the glass bottom), whereas in others where agitation and aeration took place, the particles only clustered without forming any ordered structure. Both higher-ordered and disordered structures generated through self-assembly were structurally and functionally characterized. Transmission electron microscopy (TEM) and X-ray diffraction (XRD)

Received: June 30, 2023
Revised: November 10, 2023
Accepted: November 13, 2023
Published: November 29, 2023

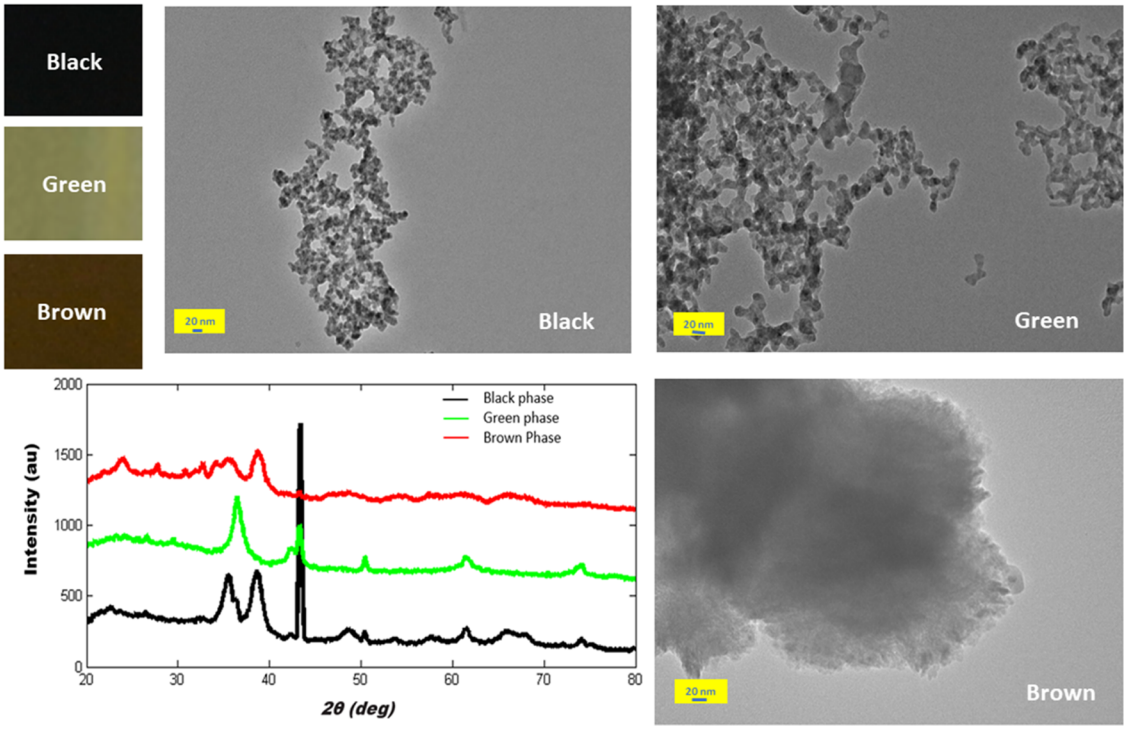

Figure 1. Relaxation behavior of the CuNPs synthesized and suspended in MQ water for a month. Immediately after the synthesis, the collected Day 0 particles appear black in color. The black color changes to green and then to brown within a month. TEM images and XRD patterns of the CuNPs withdrawn on three different days (D0, black; D15, green; and D30, brown) are also displayed here.

were performed to view the structures more closely with the preferred orientation. However, electrochemistry, catalytic activity, and hemoglobin precipitation studies were conducted to characterize the structures functionally. A loss in functional activity was found for both ordered and disordered structures in comparison to freshly prepared CuNPs.

We know that self-assembly is a process where the organization of individual components takes place to form higher-ordered structures,[9,10] and attainment of equilibrium is governed by the thermodynamically controlled processes of free energy minimization (driven by the weaker intermolecular forces between the self-assembled components). The particles synthesized by EEW technique had abundant physical and chemical processes going on during synthesis, which involved a high amount of energy storage and transfer.[11] Therefore, when the CuNPs after synthesis were kept for a month, transfer of energy fluxes within the moieties happened and energy minimization occurred, which could be the driving force for the nanowire formation.

II. MATERIALS AND METHODS

II.I. Materials. The copper nanoparticles were synthesized using a Cu (99.9%) plate and wire (0.50 mm diameter and 100 cm length) as electrodes. The DC voltage power supply was from Billionix. Milli-Q water was used (refiltered using a 0.2-μm syringe filter). Methylene blue, sodium borohydride ($NaBH_4$), and potassium ferricyanide (K_3FeCN_6/K_4FeCN_6) were purchased from Sigma-Aldrich. Potassium chloride (KCl) was from SRL company. Phosphate-buffered saline (PBS; pH 7.4) was prepared from salts (NaCl, KCl, KH_2PO_4, K_2HPO_4) from SRL company. Indium tin oxide (ITO) and the reference electrode Ag/AgCl were purchased from BASi.

II.II. Preparation and Incubation of CuNPs by EEW. CuNPs were synthesized in the presence of ultrapure Milli-Q (MQ) water (as a medium), as detailed in our previous publication.[8] The preparation was carried out with a Cu wire of 100 cm length together with a Cu plate immersed in the medium (100 mL of MQ water), as shown in Figure 1. The wire was driven through a wire guide and exploded on the Cu plate. An instantaneous current of 50A was applied at a voltage of 35 V to obtain the desired CuNP. The entire experiment was conducted inside a glass vessel; a representative image is displayed in Figure S1.

Before particle synthesis, the MQ water was filtered by a 0.2 μm syringe filter to remove any probable contaminants present in the medium. After preparation, the particles were left undisturbed in laboratory conditions for 60 min to allow the precipitation of larger particles, if any. Following separation, smaller particles in the supernatant were transferred to a fresh storage vial and used for further experiments. The collected copper nanoparticles were aliquoted at different checkpoints as and when required for detailed structural and functional analyses.

II.III. TEM and XRD Measurements. Different copper nanostructures synthesized during the study were characterized by transmission electron microscopy (TEM, JEOL 2100F, Japan) and X-ray diffraction (XRD; PANalytical 2550-PC X-ray diffractometer). For XRD, a fixed volume of aliquot was withdrawn (20 μL) from the parent vials of different solutions, such as Day 0 black, Day 15 green, and Day 30 brown CuNWs, and drop cast on glass slides (regular) separately. The action of withdrawing 20 μL of the parent sample was repeated five times to attain a measurable thin film for XRD characterization. For TEM analysis, the sample aliquot was diluted with a 3× amount of MQ water to minimize any aggregation due to high particle density. The final solution was gently mixed, and

https://doi.org/10.1021/acsomega.3c04675
ACS Omega 2023, 8, 46481−46489

20 μL of aliquot was drop cast onto a carbon-coated TEM grid for analysis, following air drying.

II.IV. Dye Reduction Assay. The catalytic activity of CuNPs was determined by a modified protocol of the dye reduction assay technique[12] using methylene blue (MB) as a substrate and sodium borohydride ($NaBH_4$) as a reducing agent. The assay was performed at room temperature (approximately 25 °C). First, 1 mL of CuNP (from 0.134 mg/mL stock) to obtain a final working concentration of 0.027 mg/mL was mixed with various amounts of MQ water (4990, 4987.5, 4985, and 4980 μL, respectively) to adjust the total volume to 5 mL, after the addition of MB and $NaBH_4$. In the respective solutions, 10 μL of 5 mM MB from the stock was added and mixed so that the final concentration of MB in the working solution became 10 μM. Then, various freshly prepared concentrations of sodium borohydride (amounts: 0, 2.5, 5, and 10 μL, respectively, from the 10 mM stock) were added into the solution, and the final concentration became 0, 5, 10, and 20 μM respectively. The addition of sodium borohydride shortens the reaction time.[13] Hence, in our case, the dye reduction took place immediately after the addition of sodium borohydride within 1−5 min. The spectral changes were recorded using a Parkin-Elmer spectrometer over the duration of 60 min in the presence of 10 μM methylene blue and 20 μM sodium borohydride, with 0.027 mg/mL CuNPs as the final concentration. In the other case, spectral changes were recorded by the consecutive addition of 2 μL of CuNPs from the 0.134 mg/mL stock using the same concentration of methylene blue (10 μM) and sodium borohydride (20 μM).

II.V. Cyclic Voltammetry Study. A 75 W 50/60 Hz, PGSTAT204, electrochemical workstation made in the Netherlands was used to characterize the CuNPs synthesized by the EEW technique. It contains a conventional three-electrode system with NOVA 1.11 software. Indium tin oxide (ITO) with 5 mm x 5 mm dimension and 10−15 Ω resistivity was used as the working electrode. As a reference electrode, Ag/Ag purchased from BASi was used, whereas a platinum sheet of 5 mm × 5 mm dimension was used as the counter electrode. The K_3FeCN_6/K_4FeCN_6 (0.3M) solution was used as the redox solution with 0.01 M KCl and 0.1 M PBS (pH = 7) as the supporting electrolyte and the main solution, respectively, for easy transport of electrons.

II.VI. Studying the Interaction of Hemoglobin. For the hemoglobin (Hb) precipitation study, a modified protocol of Ref[14] was used. 1 mL of the 0.3 mg/mL Hb stock solution was mixed with 0.5 mL of the 0.134 mg/mL CuNP stock. The final concentrations of Hb and CuNPs in the solution (1.5 mL) were 0.2 and 0.045 mg/mL, respectively. The interaction was monitored for an hour. Images were obtained immediately after the addition of CuNPs to the hemoglobin solution (time 0 denoted as $T = 0$) and after an hour (time 1 h denoted as $T = 1$ h) of reaction. A control Hb solution was prepared for reference.

For recording spectral dynamics, the concentrations of both Hb and Cu were lowered (according to an earlier study by our group[15]) to maintain the Lambert−Beer Law and avoid Cu-induced precipitation so that the spectral dynamics of Hb could be monitored without any hindrance. For this study, 3 mL of the solution was prepared with final concentrations of Hb and CuNPs of 2.15 and 45 μg/mL, respectively. The spectra were recorded at 0, 2, 5, and 10 min, respectively, immediately after mixing.

III. RESULTS

III.I. Changes in Physical Characteristics. Attainment of equilibrium or relaxation is observed through changes in the physical behavior in a system. A change in the size, shape, etc., is generally observed after a change in the environment, which indicates a relaxation behavior. Interestingly, we noticed changes in the physical properties of the CuNPs prepared by the EEW technique when kept for a month under "aerated or agitated" conditions in the same medium (shown in Figure 1). Immediately after the explosion, the synthesized CuNPs appeared black or blackish green in color (denoted as Day 0 black CuNP). To follow the relaxation behavior in detail, we collected the black CuNP (immediately after synthesis) in a 50 mL Falcon tube, aerated and agitated it, and then monitored the changes. The black particles transformed into green within the next 15 days (Day 15 green) and then became completely brown within a month (Day 30 brown). To determine the alterations more closely, TEM was performed. It was found that the freshly prepared particles, in the range of 5−20 nm,[8] are widely spread and start to rearrange themselves during the green phase. However, these particles aggregate (clusters) in the brown phase in such a way that it becomes difficult to find the individual particles. Water-induced stabilization was observed previously in the case of zinc sulfide (ZnS), prepared by the electro-explosion method and when kept in that medium (water). The authors observed structural evolution in terms of aggregation in the sample with the color changing from black to white. It took 20 days to observe these changes. They also found variation in the stoichiometry of ZnS nanoparticles when the time-lapse X-ray photoelectron spectroscopy (XPS) was measured.[16,17] Hence, it is evident that medium (water)-induced relaxation is a common phenomenon for the nanoparticles synthesized by the EEW technique.

III.II. Changes in Crystalline Properties. The CuNPs withdrawn from different phases (Day 0 black, Day 15 green, and Day 30 brown, respectively) were then subjected to XRD measurement for further analysis. Figure 1 also displays the XRD patterns of the three different phases of CuNPs. For black phase particles, the characteristic 2θ peaks appearing around 35.4, 38.6, 43.3, 49.2, 50.4, and 74.1° are attributed to (002) of CuO, (111) of CuO, (111) of Cu, (202) of CuO, (200) of Cu, and (220) of Cu, respectively. The characteristic peaks appearing around 36.4, 42.3, 43.2, 50.4, 61.4, and 74.1° in the green phase are indexed to (111) of Cu_2O, (200) of Cu_2O, (111) of Cu, (200) of Cu, (220) of Cu_2O, and (220) of Cu, respectively. The XRD peaks located around 32.7, 35.4, 38.6, and 43.2° for brown phase particles are attributed to the (110) of CuO, (002) of CuO, (111) of CuO, and (111) of Cu, respectively.[18−24] The black phase is dominated by the presence of Cu (111), reflecting the preferred orientation together with the various crystalline variants of CuO and Cu. However, in the green phase, various crystalline forms of Cu_2O are observed, but the same crystalline variants of CuO revert in the brown phase. Although all three phases contain Cu (111), the only noted observation is the reduction in the peak intensity of Cu (111) with time, which revealed that the highest number of atoms possessing the highest number of electrons in the unit cell decreases as a result of the relaxation behavior.

III.III. Electrochemistry of the CuNPs. CuNPs from different days (Day 0 black, Day 15 green, and Day 30 brown) were characterized electrochemically by cyclic voltammetry.

https://doi.org/10.1021/acsomega.3c04675
ACS Omega 2023, 8, 46481−46489

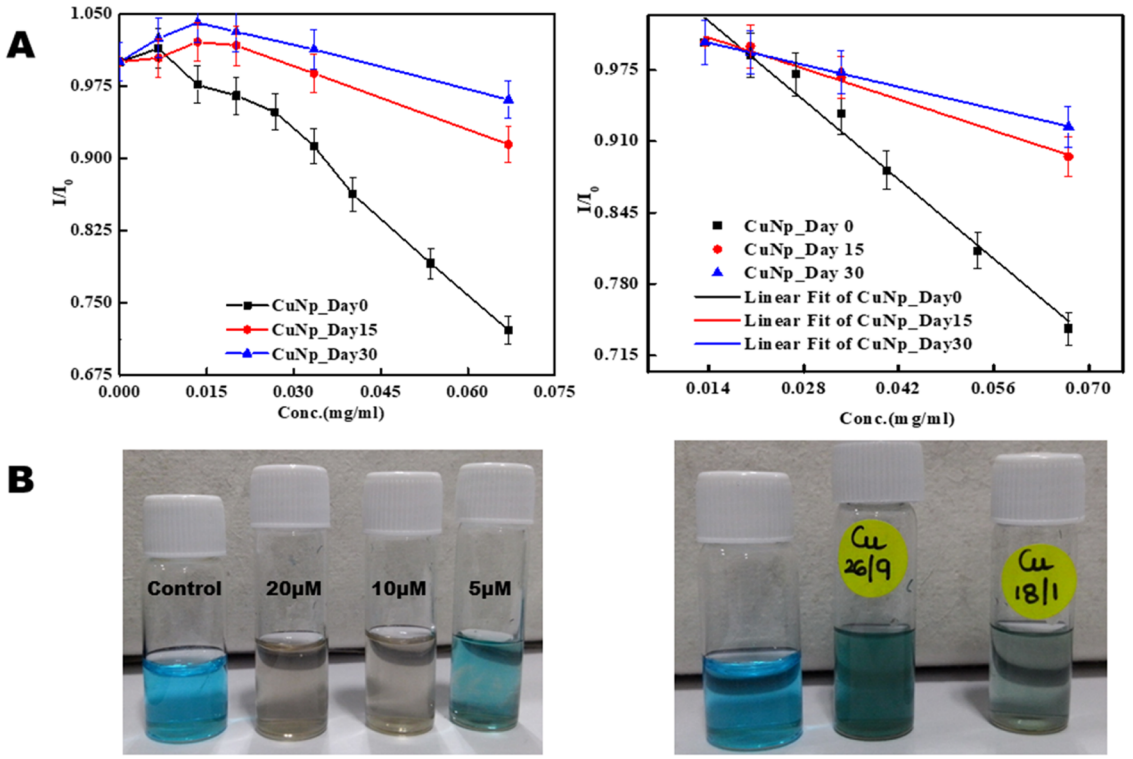

Figure 2. (A) Plot of the peak current (oxidation peak) vs concentration, extracted from the cyclic voltammetry study of the CuNPs withdrawn from Day 0 black, Day 15 green, and Day 30 brown, respectively. It is shown together with their linear fit plot on the right. (B) Catalytic activity of CuNPs in the presence of methylene blue and sodium borohydride. The image on the left shows solution mixtures of methylene blue and CuNPs after the addition of various amounts of freshly prepared sodium borohydride (20, 10, and 5 μM, respectively), and the image on the right represents the comparative catalytic activity of the Day 0 black (Cu 18/1) and Day 30 brown (Cu 26/9). The control (a solution of methylene blue) is shown at the extreme left in both images.

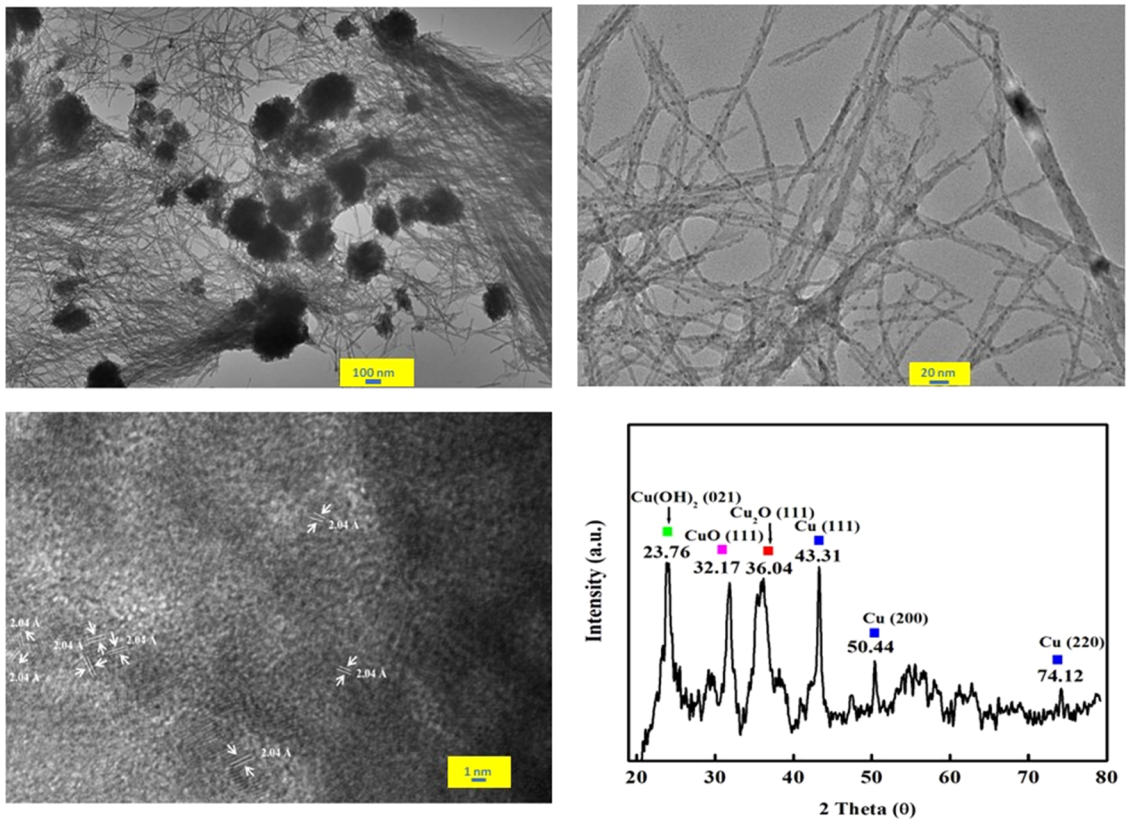

Figure 3. TEM images of the spontaneously formed Cu nanowires (CuNWs) and XRD pattern of the CuNWs.

https://doi.org/10.1021/acsomega.3c04675
ACS Omega 2023, 8, 46481−46489

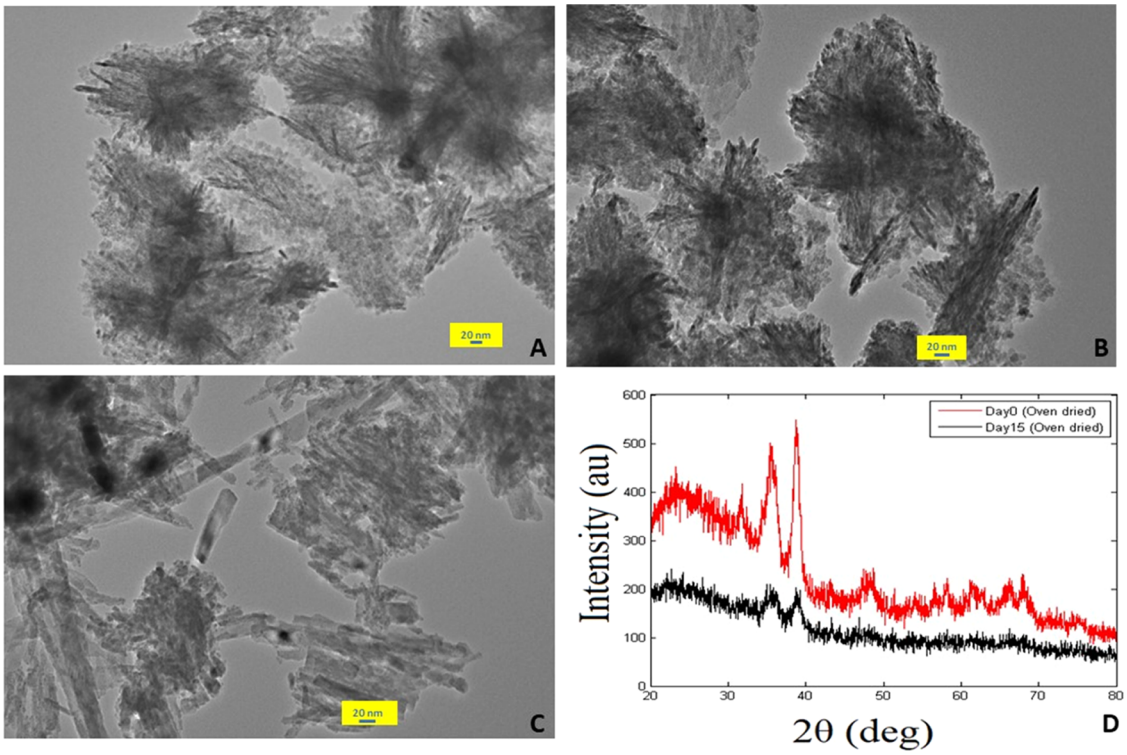

Figure 4. (A) TEM image of CuNPs from Day 0 black after thermal oxidation; (B) TEM image of CuNPs from Day 15 green after thermal oxidation; (C) TEM image of the CuNWs after thermal oxidation; and (D) XRD patterns of Day 0 black and Day 15 green CuNPs after thermal oxidation are presented as the red and black graphs, respectively.

The experiment was performed to find out the differences in the oxidation and reduction potentials of the CuNPs kept for different days to determine the changes in their electrochemical properties. Different concentrations of particles from Day 0 black, Day 15 green, and Day 30 brown were aliquoted, and the oxidation peak current was recorded with increasing concentration. The variation in the peak current against the concentration is illustrated in Figure 2A. A difference in the behavior of the oxidation peak current is observed with increasing concentrations of the same-day particles. Because of the screening effect (reaction between CuNPs and the medium), the current at the electrode decreases with increasing concentration of the CuNPs (of the same day); hence, we observe a decrease in the current.[8] However, when we consider Day 15 green and Day 30 brown CuNPs, a difference in the slopes (Table S1) was recorded (Figure 2A), which revealed that with an increase in the number of days, this screening effect is reduced, and an increase in the current at the electrode materializes. Thus, the above phenomenon explains that there is not only a physical change happening within the CuNPs with time, but their behavior also differs electronically.

III.IV. Study of the Catalytic Activity of the CuNPs. The catalytic activity of the CuNPs synthesized by the EEW technique was determined by the degradation of a cationic dye, methylene blue (MB). Copper nanoparticles were tested for their catalytic activity using MB as the substrate and sodium borohydrate ($NaBH_4$) as the reducing agent. MB has two characteristic peaks in its absorption spectrum. The primary absorption peak for MB is observed at 664 nm, and a secondary peak is observed at 292 nm.[12] It was noticed that in the presence of various concentrations of sodium borohydride (0, 5, 10, and 20 μM) and methylene blue, the CuNPs from Day 0 black decolorize the entire solution within 1−5 min (Figure 2B, left image). This colorless form of methylene blue is known as leuco-methylene blue (LMB), which is a reduced form of MB. LMB exhibits a characteristic absorption peak at 256 nm.[25] The spectral representation of the time kinetics and concentration-dependent events is shown in Figure S2. To test the catalytic properties of freshly synthesized CuNPs (Day 0 black) and CuNPs from Day 30 brown, the redox reaction of MB was exploited in the presence of sodium borohydride. The observation is depicted in Figure 2B (right image). In the figure, the black CuNPs (Cu 18/1) were able to decolorize the dye MB to the colorless form LMB, but the brown phase CuNPs (Cu 26/9) were unable to decolorize it fully, and the kinetics was also found to be slower than that of Day 0 CuNPs.

III.V. Formation of Cu Nanowires (CuNWs) from CuNPs Prepared by the Electro-Explosion Technique. We also observed an unusual behavior of the CuNPs synthesized by the EEW technique when kept for a month in a glass vessel without any "agitation and aeration". These CuNPs arranged themselves into tangled wires at the bottom of the vessel on a glass support through self-assembly.

TEM and HRTEM images of the CuNWs formed from the CuNPs are shown in Figure 3. When the black CuNPs, immediately after synthesis, were collected in water as the medium (in a 50 mL glass bottle) for a month, without any agitation and aeration, the formation of wires was noted. After characterization through TEM, it was found that the length of the wires was in millimeters, but their width varied from 3.3 to 20 nm (Figure S3). The interplanar spacing of 0.204 nm corresponding to the (111) plane of the FCC copper confirms the presence of the metal (revealed by HRTEM).[26] Additionally, affirming our observations from XRD, the grown nanowires show a growth preference in the (110) plane.

https://doi.org/10.1021/acsomega.3c04675
ACS Omega 2023, 8, 46481−46489

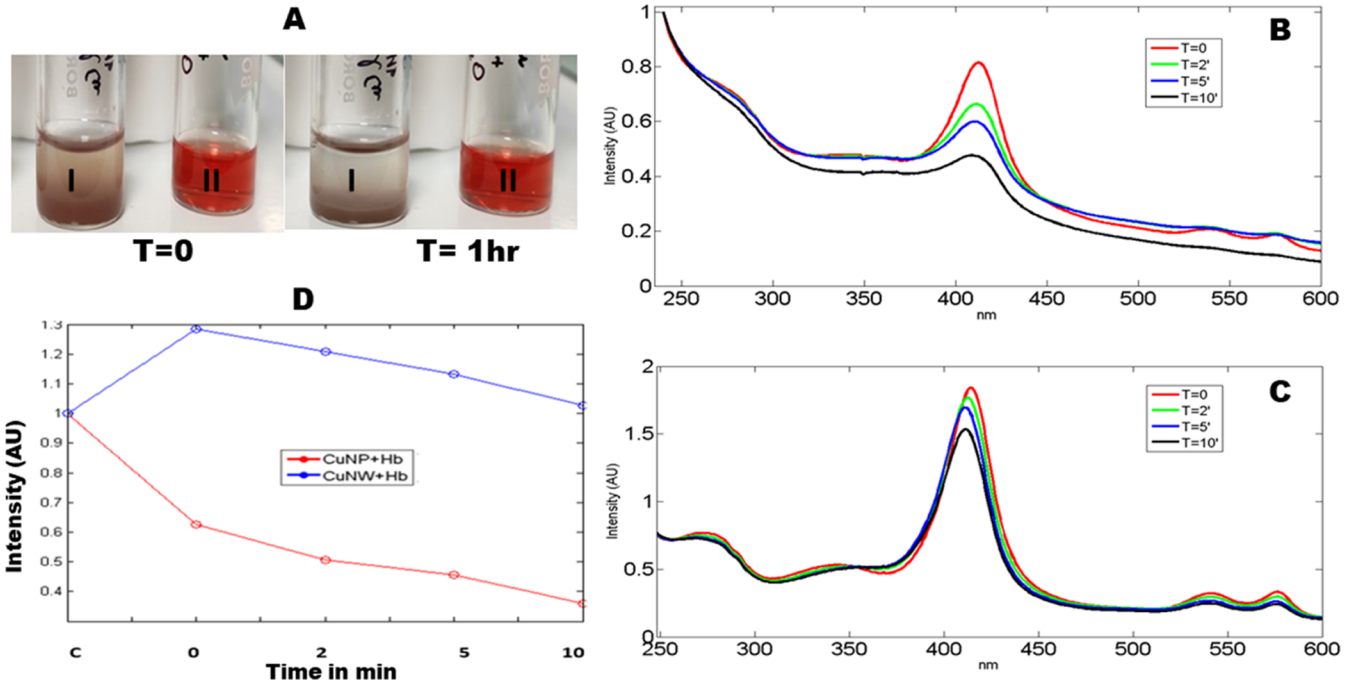

Figure 5. (A) (I, II) CuNP-dependent precipitation study of hemoglobin (Hb), where $T = 0$ and $T = 1$ h represent Hb mixed with CuNPs at time 0 and after time 1 h, respectively. The Hb solution as a control is also shown in both I and II. (B, C) UV−vis spectra of hemoglobin after the addition of CuNP D0 black and CuNWs, respectively. (D) Dynamics of the Soret band (415 nm) from (B) and (C) are plotted and represented at 0, 2, 5, and 10 min. The 415 nm OD of only hemoglobin (control) as a starting point is shown (C, in the *x*-axis) in the graph.

Notably, HRTEM is also marked by the presence of prominent twinning boundaries running throughout the length of the nanowires. The twin could arise due to the directional plane shift during the synthesis; however, the *d* spacing in either direction is estimated to be of the same value, which is 0.20 nm, indicating the polycrystalline nature of the grown nanowires. Multi-twinned seed nanostructures are rather common to form and can grow larger in size; however, beyond a critical size, they tend to grow one-dimensionally in a parallel axis to overcome strain, explaining the growth mechanism of the CuNW sample.[27] Polycrystallinity can be introduced or retarded by using different surfactants, polymers, or reaction conditions. In the reported method, as no chemicals are used, room temperature can be ascribed to be a possible driver of polycrystal seeds due to the retarded thermodynamic diffusion at low temperatures.[28] In summary, retarded thermodynamic diffusion forms multi-twinning seed nanostructures that grow in size up to a threshold value, drifting to adopt 1D growth to attain thermodynamic stability and the energy requirements of a stable system.

Representative XRD patterns for the above nanowire sample are also shown in Figure 3. The recorded peaks in the spectrum at 43.31, 50.44, and 74.12° index well to the typical (111), (200), and (220) reflections of the face-centered cubic Cu structure (JCPDS 85-1326). Of the three planes, (111) with the highest intensity is indicative of the preferred orientation of the grown structures. Inevitability, the formation of copper oxide on the copper nanostructure surface results in additional reflections at 23.76, 31.77, and 36.17°. The peaks, in order, represent the (021) plane of $Cu(OH)_2$ and (111) of CuO and Cu_2O.[29,30] The presence of the surface copper oxide layer is consequential to the reaction of copper with oxygen in the air within the vessel and the dissolved oxygen in the solvent.

III.VI. Characterization of CuNPs and CuNWs after Thermal Oxidation. The CuNPs from the D0 black, D15 green, and CuNW solutions were thermally oxidized to determine the effects on their chemical composition and integrity.[31] The solutions were kept at 60 °C in airy conditions to let the solutions dry. After drying, the vials were taken out from the oven and analyzed. All three samples turned brown after oxidation. The TEM images of the samples are displayed in Figure 4A−C. Particle aggregation with the formation of rod-shaped structures is observed in CuNPs from D0 black. Similar observations are made with D15 green samples, but compared to D0 black samples, a higher number of rod-shaped structures is noted. In the case of CuNWs, it is observed that the lengthy wires are broken into small pieces of rods.

The Bragg reflection of thermally oxidized CuNPs from D0 black is recorded at 31.8° ((110) of CuO), 35.46° ((002) of CuO, cubic symmetry phase), 38.794° ((111)/(200) of CuO), 48.793° ((2, 0, −2) of CuO), and 66.184° ((311) of CuO), whereas for CuNPs from D15 green, the Bragg reflection is recorded at 35.46° ((002) of CuO cubic symmetry), 38.6° ((111) of CuO), and 66.2° ((311) of CuO).

III.VII. Comparative Study of the Interaction between Hemoglobin and CuNPs or CuNWs, Respectively. We observed the precipitation of the blood protein hemoglobin (Hb) by CuNPs prepared by the EEW technique, as displayed in Figure 5A. The figure represents two cases, I and II. I shows a mixture of Hb and CuNPs at time 0 ($T = 0$) and after an hour ($T = 1$ h). However, II represents only the Hb solution used throughout as the control. The Hb solution in (I) starts to precipitate as soon as CuNPs are added to the sample, and within an hour, a clear solution appears as a result of Hb−CuNP assembly at the bottom. A dynamic light scattering (DLS) study by our group earlier showed that CuNPs prepared by this technique increase the size of the Hb by

https://doi.org/10.1021/acsomega.3c04675
ACS Omega 2023, 8, 46481−46489

the formation of clusters, leading to aggregation followed by precipitation.[14]

In the current study, we compared the strength of interaction of Hb with CuNP Day 0 black and CuNWs by measuring the heme spectra of Hb using UV−vis spectroscopy (illustrated in Figure 5B,C). Earlier, we monitored characteristic spectral shifts of Hb at the Soret region (408−420 nm) in the presence of various ligands,[15] indicating differences in the stress response of ligands. Additionally, a noticeable decrease in the Soret band intensity or complete removal of the heme group was noted as a result of secondary structure transitions.[32] Thus, to compare the interaction strengths of these two forms of Cu (particles and wires), we decided to compare the periodic dynamics of Hb spectra in the Soret region. The heme spectra recorded at T = 0, 2, 5, and 10 min depict the time intervals at which the spectra were obtained. This shows that the Soret band traverses to the lower wavelength with a loss in intensity in the case of both particles and wires, but the interaction is much stronger in CuNPs than in CuNWs as the former aggressively changes the spectral dynamics (OD @ 415 nm decreases from the very beginning), leading to heme release and protein aggregation (revealed by the increase in the absorption of the baseline in the red region, 625−750 nm)[33] and also seen in the image in Figure 5A. In addition, the peaks at 540 and 570 nm, representing the oxygen-bound form of Hb,[34] completely disappeared, whereas they were found to be still present in the case of the latter (CuNWs) even after 10 min, indicating that the oxygen molecules were not completely removed from the heme iron due to the mild interaction of CuNWs. Figure 5D shows the above incidence (intensity @ 415 nm vs time plot) in the normalized graphical form. The control Hb spectra are not shown in parts (B) and (C) for clarity, but they are shown in (D) as the starting point (C) in the X-axis to present the differences in the trajectories.

IV. DISCUSSION

Electro-explosion of wire (EEW) is a physical and environmentally friendly technique. It is currently being investigated to synthesize nanoparticles with less contamination because the nanoparticles are formed by exploding a pure metal wire. Many parameters control the process of synthesis, such as the wire dimension, medium, current density, type of metal, etc. As a huge amount of energy is also associated with the synthesis, we noticed some interesting phenomena in the nanoparticles. In our work, when CuNPs produced by the EEW technique were stored in the medium (water) for a month, two kinds of phenomena took place: first, the emergence of higher-disordered structures, such as aggregates or clusters, and second, nanowire formation. This structural organization (self-assembly) happened independently; the only difference was that in the former, the system was disturbed by aeration and/or agitation, whereas in the latter, the system was not disturbed. It is reported that factors such as mass transport, reversibility, environment, and interplay of intermolecular forces (such as Vander Waals and Coulomb interactions) influence the self-assembly process.[35] As the CuNPs synthesized by the EEW technique did not require any external driving force and were dependent only on the physical and/or chemical interactions to form the nanowires, the intermolecular forces acting on the CuNPs should have balanced the resultant forces and helped in the self-assembly process to form nanowires. A balance between the attractive and repulsive forces within the moieties (components) is important. If the components strongly stick together (which happens when the attractive force is stronger), there remains no provision for the formation of an ordered structure, and aggregation is observed (e.g., Day 30 brown phase). On the other hand, if the components can adjust their positions by bond breaking and formation (when forces act differentially), an ordered structure (e.g., CuNWs) is anticipated.[36] Thus, we observed the formation of both a disordered structure (clusters) and an ordered structure (CuNWs) depending on the conditions.

We also noticed that the bare metallic CuNPs synthesized by the EEW technique, after some time, tend to aggregate and precipitate, which might have happened as a consequence of collisions due to Brownian motion, gravity, or differential settling.[37] Several strategies such as evaporation, interface assembly, printing, patterning, and pressure-driven assembly mechanisms are well-known to control the environment externally in order to obtain higher-ordered structures such as nanowires.[38,39] Crowding-induced self-assembly influenced by Brownian motion and or gravity (applicable when the components grow in size) is also another strategy, which is not a very common process to grow nanowires. However, considering the time scale (>1 month) of the nanowire formation in our case, there is a high possibility of this mechanism to prevail.[40,41]

For static self-assembly (which happens in our system as there is no external driving force), energy minimization also drives the formation of the self-assembled structure.[42] As the CuNPs discussed here are the result of enforcement of a high amount of energy, they should possess a tendency to stabilize themselves by energy minimization that might facilitate the self-assembly process.

In summary, our research provided experimental evidence that not all equilibrium state attainments generate ordered molecular structures. Although a loss of functionality (catalytic, electrochemical activity, or interaction with protein) in both cases (ordered or aggregated) was noticed, to decipher the exact process of formation of this higher-ordered structure, especially nanowires, a close monitoring of the association between the moieties is required. Studying the process of static or directed self-assembly is currently important for fabricating 3D structures or devices. Cu maintains its excellent price-to-performance ratio while offering similar electrical, thermal, and mechanical properties as compared to silver (Ag) and gold (Au) and is the most widely used metal in various industries, especially electronics.[43] On the other hand, CuNW-based flexible transparent electrodes (FTEs) play a crucial role in a range of optoelectrical devices from solar cells, touch screens, and organic light-emitting diodes [OLEDs][44,45] to wearable electronics and bendable sensors.[46] The low sheet resistance, easy tensile bending, and superior electrical conductivity of the nanowires have helped in the fabrication of low-cost and high-performance flexible electronic devices.[43] It was demonstrated that achieving ultralong CuNWs with a high aspect ratio is crucial for obtaining FTEs with exceptional performance.[42] The presence of mixed particles and surface oxidation in CuNWs can significantly degrade both transmittance and conductivity.[43] Therefore, the production of highly purified CuNWs needs a more controlled environment and attention. However, the synthesis of these CuNWs often involves a tedious process and necessitates the use of external forces or additional compounds to initiate wire synthesis. In contrast,

https://doi.org/10.1021/acsomega.3c04675
ACS Omega 2023, 8, 46481−46489

our work delves deeper into the fundamental self-assembly mechanism. These spontaneous self-assembly processes can be more cost-effective than traditional manufacturing methods, especially for producing large quantities of nanoscale materials. Besides, it eliminates the use of additional compounds in manufacturing and can become a more effective synthesis method.

In our study, we primarily focused on the formation of CuNWs from CuNPs by a self-assembly process because not only is understanding the resulting properties of the nanowires important for the above reasons, but investigating the mechanism of the process might also provide insights into the fundamental principles of nanoscale self-organization, which will eventually contribute in different fields of nanotechnology such as nanomaterials and nanoelectronics[44] and open up a new direction for utilizing nanoparticles prepared by the top−down method of the exploding wire technique for the fabrication of higher-ordered structures by the bottom−up approach.

■ ASSOCIATED CONTENT

Supporting Information

The Supporting Information is available free of charge at https://pubs.acs.org/doi/10.1021/acsomega.3c04675.

An image of the EEW reaction vessel and components, values extracted from the slopes corresponding to Figure 2A, detailed spectral representation of methylene blue (time kinetics and concentration-dependent events), and measured width values of nanowires from the HRTEM image (PDF)

■ AUTHOR INFORMATION

Corresponding Author

Ranjita Ghosh Moulick − *Amity Institute of Biotechnology/Amity Institute of Integrative Sciences and Health, Amity University Haryana, Gurugram 122413 Haryana, India;* orcid.org/0000-0003-1890-8458; Email: ranjita.ghoshmoulick@gmail.com

Authors

Subhavna Juneja − *School of Biotechnology, Jawaharlal Nehru University, New Delhi 110067, India;* Present Address: Engineering Photonics Research Laboratory, Electrical Engineering and Computer Science, College of Engineering, Oregon State University, Corvallis, Oregon 97331, United States

Jagriti Gupta − *School of Environmental Sciences, Jawaharlal Nehru University, New Delhi 110067, India*

Vaishali Rana − *Amity Institute of Biotechnology/Amity Institute of Integrative Sciences and Health, Amity University Haryana, Gurugram 122413 Haryana, India*

Jaydeep Bhattacharya − *School of Biotechnology, Jawaharlal Nehru University, New Delhi 110067, India;* orcid.org/0000-0001-7268-0867

Complete contact information is available at: https://pubs.acs.org/10.1021/acsomega.3c04675

Notes

The authors declare no competing financial interest.

■ ACKNOWLEDGMENTS

The authors are extremely thankful to Prof. Prasenjit Sen (Retd., Jawaharlal Nehru University, New Delhi, India) for his valuable insights while performing the experiments and to Susaritha, Mini Agrawal, Jyoti Bisht, and Ahana Mukherjee for their help during the experiments and writing. The authors also thank the funding agencies DST (TDP/BDTD/25/2019), DBT (BT/PR36285/NNT/28/2019), and ICMR (56/4/2020/Hae/BMS) of India.

■ REFERENCES

(1) Sen, P.; Ghosh, J.; Abdullah, A.; Kumar, P.; Vandana. Preparation of Cu, Ag, Fe and Al nanoparticles by the exploding wire technique. *J. Chem. Sci.* **2003**, *115*, 499−508.

(2) Ranjan, P.; Nguyen, D. H.; Chen, L.; Cotton, I.; Suematsu, H.; Chakravarthy, S. R.; Jayaganthan, R.; Sarathi, R. Dynamical aspects of nanoparticle formation by wire explosion process. *Nano Express* **2020**, *1* (1), No. 010049.

(3) Kotov, Y. A. Electric explosion of wires as a method for preparation of nanopowders. *J. Nanopart. Res.* **2003**, *5*, 539−550.

(4) Lázár, K.; Varga, L. K.; Kis, V. K.; Fekete, T.; Klencsár, Z.; Stichleutner, S.; Szabó, L.; Harsányi, I. Electric Explosion of Steel Wires for Production of Nanoparticles: Reactions with the Liquid Media. *J. Alloys Compd.* **2018**, *763*, 759−770.

(5) Nazarenko, O. B.; Ilyin, A. P. In *Nano Powders Production by Electrical Explosion of Wires: Environmental Applications*, Proceedings of the 3rd Environmental Physics Conference, 2008.

(6) Kwon, Y.-S.; Gromov, A. A.; Ilyin, A. P.; Rim, G.-H. Passivation Process for Superfine Aluminum Powders Obtained by Electrical Explosion of Wires. *Appl. Surf. Sci.* **2003**, *211* (1−4), 57−67.

(7) Bac, L. H.; Kim, J. S.; Kim, J. C. Size, Optical, and Stability Properties of Gold Nanoparticles Synthesized by Electrical Explosion of Wire in Different Aqueous Media. *Rev. Adv. Mater. Sci.* **2011**, *28*, 117−121.

(8) Gupta, J.; Bisht, J.; Agrawal, M.; Bhattacharya, J.; Sen, P.; Moulick, R. G. A method to detect immunoreactions on the basis of current vs. concentration slope−an electrochemical approach. *RSC Adv.* **2020**, *10* (73), 44798−44804.

(9) Grzelczak, M.; Vermant, J.; Furst, E. M.; Liz-Marzán, L. M. Directed self-assembly of nanoparticles. *ACS Nano* **2010**, *4* (7), 3591−3605.

(10) Lin, Y.; Böker, A.; He, J.; Sill, K.; Xiang, H.; Abetz, C.; Russell, T. P.; et al. Self-directed self-assembly of nanoparticle/copolymer mixtures. *Nature* **2005**, *434* (7029), 55−59.

(11) Han, R.; Li, C.; Yuan, W.; Ouyang, J.; Wu, J.; Wang, Y.; Ding, W.; Zhang, Y. Experiments on plasma dynamics of electrical wire explosion in air. *High Voltage* **2022**, *7* (1), 117−136.

(12) Singh, J.; Juneja, S.; Soni, R. K.; Bhattacharya, J. Sunlight-Mediated Enhanced Photocatalytic Activity of TiO2 Nanoparticles Functionalized CuO-Cu2O Nanorods for Removal of Methylene Blue and Oxytetracycline Hydrochloride. *J. Colloid Interface Sci.* **2021**, *590*, 60−71.

(13) Kassem, A. A.; Abdelhamid, H. N.; Fouad, D. M.; Ibrahim, S. A. Hydrogenation Reduction of Dyes Using Metal-Organic Framework-Derived CuO@C. *Microporous Mesoporous Mater.* **2020**, *305*, No. 110340.

(14) Bhattacharya, J.; Choudhuri, U.; Siwach, O.; Sen, P.; Dasgupta, A. K. Interaction of hemoglobin and copper nanoparticles: implications in hemoglobinopathy. *Nanomed.: Nanotechnol. Biol. Med.* **2006**, *2* (3), 191−199.

(15) Bhattacharya, J.; Ghosh Moulick, R.; Choudhuri, U.; Bhattacharya, P. K.; Lahiri, P.; Chakrabarti, B.; Dasgupta, A. Lazy dynamics of unfolding and ligand interaction-signatures in hemoglobin and its glycated form. *Indian J. Phys.* **2004**, *78B*, 55−63.

(16) Goswami, N.; Sen, P. Water-induced stabilization of ZnS nanoparticles. *Solid State Commun.* **2004**, *132* (11), 791−794.

(17) Goswami, N.; Sen, P. Water driven stabilization of ZnS nanoparticles prepared by exploding wire technique. *Mater. Res. Express* **2014**, *1* (2), No. 025001.
(18) Arya, S.; Singh, A.; Kour, R. Comparative Study of CuO, CuO@Ag, and CuO@Ag: La Nanoparticles for Their Photosensing Properties. *Mater. Res. Express* **2019**, *6* (11), No. 116313.
(19) Rahman, A.; Ismail, A.; Jumbianti, D.; Magdalena, S.; Sudrajat, H. Synthesis of Copper Oxide Nanoparticles by Using Phormidium Cyanobacterium. *Indonesian J. Chem.* **2009**, *9* (3), 355−360.
(20) Akgul, F. A.; Akgul, G.; Yildirim, N.; Unalan, H. E.; Turan, R. Influence of Thermal Annealing on Microstructural, Morphological, Optical Properties, and Surface Electronic Structure of Copper Oxide Thin Films. *Mater. Chem. Phys.* **2014**, *147* (3), 987−995.
(21) Sukumar, S.; Rudrasenan, A.; Nambiar, D. P. Green-Synthesized Rice-Shaped Copper Oxide Nanoparticles Using Caesalpinia bonducella Seed Extract and Their Applications. *ACS Omega* **2020**, *5* (2), 1040−1051.
(22) Zhu, D.; Wang, L.; Yu, W.; Xie, H. Intriguingly High Thermal Conductivity Increment for CuO Nanowires Contained Nanofluids with Low Viscosity. *Sci. Rep.* **2018**, *8* (1), No. 5282.
(23) Jing, C.; Yan, C.-J.; Yuan, X.-T.; Zhu, L.-P. Biosynthesis of Copper Oxide Nanoparticles and Their Potential Synergistic Effect on Alloxan-Induced Oxidative Stress Conditions during Cardiac Injury in Sprague−Dawley Rats. *J. Photochem. Photobiol. B* **2019**, *198*, No. 111557.
(24) Yang, Y.; Xu, D.; Wu, Q.; Diao, P. Cu2O/CuO Bilayered Composite as a High-Efficiency Photocathode for Photoelectrochemical Hydrogen Evolution Reaction. *Sci. Rep.* **2016**, *6* (1), No. 35158.
(25) Lee, S. K.; Mills, A. Novel photochemistry of leuco-Methylene Blue. *Chem. Commun.* **2003**, No. 18, 2366−2367.
(26) Ravi Kumar, D. V.; Kim, I.; Zhong, Z.; Kim, K.; Lee, D.; Moon, J. Cu (II)−alkyl amine complex mediated hydrothermal synthesis of Cu nanowires: exploring the dual role of alkyl amines. *Phys. Chem. Chem. Phys.* **2014**, *16* (40), 22107−22115.
(27) Wang, Y.; Jiang, X.; Herricks, T.; Xia, Y. Single crystalline nanowires of lead: Large-scale synthesis, mechanistic studies, and transport measurements. *J. Phys. Chem. B* **2004**, *108* (25), 8631−8640.
(28) Shi, Y.; Li, H.; Chen, L.; Huang, X. Obtaining ultra-long copper nanowires via a hydrothermal process. *Sci. Technol. Adv. Mater.* **2005**, *6* (7), 761−765.
(29) Kanase, R. S.; Kang, S. H. Effect of KHCO 3 Concentration Using CuO Nanowire for Electrochemical CO 2 Reduction Reaction. *J. Microelectron. Packag. Soc.* **2020**, *27* (4), 11−17.
(30) Khan, A.; Rashid, A.; Younas, R.; Chong, R. A chemical reduction approach to the synthesis of copper nanoparticles. *Int. Nano Lett.* **2016**, *6*, 21−26.
(31) Krajewski, M.; Brzozka, K.; Tokarczyk, M.; Kowalski, G.; Lewinska, S.; Slawska-Waniewska, A.; Lin, H. M.; Lin, H. M. Impact of thermal oxidation on chemical composition and magnetic properties of iron nanoparticles. *J. Magn. Magn. Mater.* **2018**, *458*, 346−354.
(32) Ghosh Moulick, R.; Bhattacharya, J.; Roy, S.; Basak, S.; Dasgupta, A. K. Compensatory secondary structure alterations in protein glycation. *Biochim. Biophys. Acta* **2007**, *1774* (2), 233−242.
(33) Rana, V.; Mukherjee, A.; Basnal, Y.; Kushwaha, D.; Bhattacharya, J.; Moulick, R. G. Determination of hemoglobin-derived advanced glycation end products deploying metal salts in solution: Towards development of low-cost detection technique. *J. Mol. Liq.* **2022**, *366*, No. 120338.
(34) Robles, F. E.; Chowdhury, S.; Wax, A. Assessing hemoglobin concentration using spectroscopic optical coherence tomography for feasibility of tissue diagnostics. *Biomed. Opt. Express* **2010**, *1* (1), 310−317.
(35) Saywell, A.; Magnano, G.; Satterley, C. J.; Perdigão, L. M.; Britton, A. J.; Taleb, N.; Beton, P. H.; et al. Self-assembled aggregates formed by single-molecule magnets on a gold surface. *Nat. Commun.* **2010**, *1* (1), No. 75.
(36) Whitesides, G. M.; Boncheva, M. Beyond molecules: Self-assembly of mesoscopic and macroscopic components. *Proc. Natl. Acad. Sci. U.S.A.* **2002**, *99* (8), 4769−4774.
(37) Camassa, R.; Harris, D. M.; Hunt, R.; Kilic, Z.; McLaughlin, R. M. A first-principle mechanism for particulate aggregation and self-assembly in stratified fluids. *Nat. Commun.* **2019**, *10* (1), No. 5804.
(38) Chen, Y.; Liang, T.; Chen, L.; Chen, Y.; Yang, B.; Luo, Y.; Liu, G. Self-assembly, alignment, and patterning of metal nanowires. *Nanoscale Horiz.* **2022**, *7*, 1299.
(39) He, Z.; Wang, J.; Chen, S.; Liu, J.; Yu, S. Self-Assembly of Nanowires: From Dynamic Monitoring to Precision Control. *Acc. Chem. Res.* **2022**, *55* (11), 1480.
(40) Lash, M. H.; Fedorchak, M. V.; McCarthy, J. J.; Little, S. R. Scaling Up Self-Assembly: Bottom-Up Approaches to Macroscopic Particle Organization. *Soft Matter* **2015**, *11* (28), 5597−5609.
(41) Wei, W.; Bai, F.Self-Assembly of Nanoparticles. In *Synthesis and Applications of Optically Active Nanomaterials*; World Scientific, 2017; Vol. *14*, pp 1−56.
(42) Ozin, G. A.; Hou, K.; Lotsch, B. V.; Cademartiri, L.; Puzzo, D. P.; Scotognella, F.; Ghadimi, A.; Thomson, J. Nanofabrication by self-assembly. *Mater. Today* **2009**, *12* (5), 12−23.
(43) Li, X.; Wang, Y.; Yin, C.; Yin, Z. Copper Nanowires in Recent Electronic Applications: Progress and Perspectives. *J. Mater. Chem. C* **2020**, *8* (3), 849−872.
(44) Zhang, Y.; Guo, J.; Xu, D.; Sun, Y.; Yan, F. Synthesis of Ultralong Copper Nanowires for High-Performance Flexible Transparent Conductive Electrodes: The Effects of Polyhydric Alcohols. *Langmuir* **2018**, *34* (13), 3884−3893.
(45) Zhang, H.; Wang, S.; Tian, Y.; Wen, J.; Hang, C.; Zheng, Z.; Huang, Y.; Ding, S.; Wang, C. High-Efficiency Extraction Synthesis for High-Purity Copper Nanowires and Their Applications in Flexible Transparent Electrodes. *Nano Mater. Sci.* **2020**, *2* (2), 164−171.
(46) Amadi, E. V.; Venkataraman, A.; Papadopoulos, C. Nanoscale Self-Assembly: Concepts, Applications, and Challenges. *Nanotechnology* **2022**, *33* (13), No. 132001.

https://doi.org/10.1021/acsomega.3c04675
ACS Omega 2023, 8, 46481−46489